Experimental study of a round jet in cross-flow by means of PIV

Gennaro Cardone, Francesco G. Nese and T. Astarita
Dipartimento di Energetica TErmofluidodinamica applicata e Condizionamenti Ambientali DETEC,
Università di Napoli
p.le Tecchio, 80-80125, Naples
ITALY
gcardone@unina.it http://www.detec.unina.it

Abstract: This paper reports on results from PIV measurements in a round jet in cross-flow. The Reynolds number based on free stream velocity and jet diameter is 8000. The study is restricted to jet to stream velocity ratios ranging from 1 to 5. The vortical structures originating from the interaction of the jet with the cross-flow are visualized and the mean velocity fields and the turbulent shear stresses are measured. Measurements are performed in the symmetry plane and in planes normal to the jet axis. Results are in good agreement with data reported in the literature by other authors.

Keywords: Visualization, PIV, Jet in cross-flow, Turbulence

1. Introduction

Jets in cross-flow are of great relevance in a lot of engineering applications, such as film cooling in turbine blades, jets in combustors and waste disposal into water bodies and in the atmosphere. As reported by many authors, the behavior of the jet depends mainly on the jet to free stream velocity ratio R and on the Reynolds number, based on free stream velocity and jet diameter.

Many authors carried out experimental investigations of a jet in cross-flow; Andreopoulos and Rodi [1] used a triple hot wire probe to measure the mean and fluctuating velocities components.
Kelso et al. [2] carried out a flying-hot-wire study and a flow visualization study employing dye tracers in a water tunnel.

The visualizations show many vortical structures which originate from the interaction of the jet with the cross-flow. For Re <1600, horseshoe vortices were observed on the upstream side of the jet and on its lateral edges near the wall; for Re>1600, no occurrence of such a steady vortex system was found. Ring-like vortices typical of free jets which originate from the jet shear layer were observed on both the lateral edges of the jet. Wall vortices which develop near the wall downstream of the jet and the upright vortices generated from the interaction of the jet with the wall boundary layer were also detected. The bending over of the jet forms a counter-rotating vortex pair which becomes the dominant flow feature and persists far downstream.

Sykes et al.[3] and Coelho and Hunt [4] made mostly numerical simulations which were in good agreement with their own experimental measurements; the latter authors used an inviscid three-dimensional vortex-sheet model. Yuan et al. [5] performed a series of large eddy simulations, in which they computed the flow of a round turbulent jet issuing into a laminar boundary layer and discussed the rich variety of coherent vortical structures in the near field of the jet. They made the simulations for Reynolds numbers of 1050 and 2100, and for jet to cross flow velocity ratios of 2.0 and 3.3.

Measurements available in the literature exhibit several limitations, in fact hot-wire anemometry can give large errors in regions of high turbulent kinetic energy, are insensitive to the flow direction and, as the laser Doppler anemometry, gives only point-measurements. More recent measurements obtained by Particle Image Velocimetry (PIV) do not have these limitations and allow to obtain hundreds of independent velocity vectors at the same time. PIV measurements have been recently performed by Meyer et al. [6] for a Reynolds number equal to 2400 and R=3.3.

The main purpose of this work is to extensively analyze the velocity field at a higher Reynolds number in the proximity of the jet so as to better understand the phenomenology of a jet in cross-flow and to produce a high reliability database

which can be used to validate numerical codes.

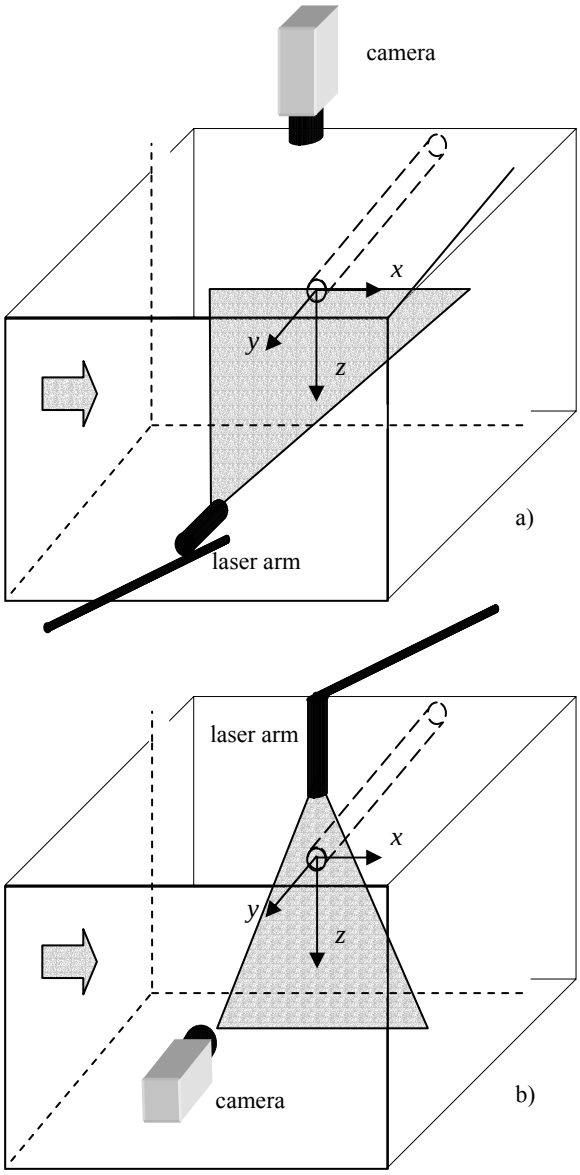

Fig.1 - Schematic view of the experimental apparatus. a) measurements in the symmetry plane; b) measurements in the planes normal to the jet axis.

2. Experimental set-up

Experiments are carried out in a subsonic wind tunnel with a rectangular test section 300x400mm^2. The turbulence intensity level in the tunnel test section is about 0.1%. The jet issues from a cylindrical nozzle, having an exit diameter D=24mm, placed on the centerline of the 300mm side. The Reynolds number based on jet diameter and free-stream velocity is 8000. In order to reach such a Re, the free-stream velocity u_∞ is set to 5m/s, the jet exit velocity V_j ranges from 5 to 25m/s, obtaining velocity ratios $R=V_j/u_\infty$ ranging from 1 to 5. Seeding made up of oil droplets, about 1μm in diameter (Somerscales [7]), is injected into the main flow and into the jet flow. The light sheet is generated by a double cavity Nd-YAG laser, while the PIV images are recorded with a PCO-Sensicam camera using an f-number of 2.8.

The schematic view of the experimental apparatus with the positions of the laser arm and the camera and the adopted coordinate system are shown in figure 1. For each value of the velocity ratio, 500 images are taken with an acquisition rate of 2Hz and both the instantaneous and the mean velocity field are computed in the z=0 centerplane (see Fig. 1a), where the flow is symmetric. The same type of acquisition is performed for planes normal to the jet at y/D=0.25, y/D=0.5, y/D=1, y/D=1.5 and y/D=2 (see Fig. 1b). The acquired images are interrogated by a super resolution PIV algorithm briefly described in the following. This method first calculates the cross-correlation of two homologous windows, in which each image is subdivided. The cross-correlation is performed with the classical FFT algorithm in order to reduce the computational burden. Once the cross-correlation map is obtained, a peak detection operation is performed over the map to determine the precise location of the peak through a sub-pixel interpolation routine. In this way it is possible to compute a preliminary displacement field of the particles in the whole image. The method then makes use of a translation, a rotation and a deformation of the interrogation windows. In turn such a predicted displacement is corrected by means of an iterative procedure. In addition, while iterating the algorithm allows a refinement of the size of the interrogation areas. In the present experiments, the starting area linear dimension is of 64 pixels and the final one of 16 pixels. Furthermore, the quality of the measured vectors is controlled with a data validation criterion applied at each intermediate step of the iteration process. This criterion compares each vector with the others in the neighborhood with a statistical method: a vector is considered affected by error if it maintains a fixed degree of continuity with those nearby it, otherwise, it has to be substituted with another one calculated by a bilinear interpolation.

3. Results

Figures 2 to 6 show results of measurements averaged over 500 values for the five tested velocity ratios. The Cartesian coordinate system is the one

shown in figure 1. The spatial coordinates are non-dimensionalized by the nozzle exit diameter D, the mean velocity components by the cross-flow velocity u_∞, the turbulent shear stresses and the turbulent intensity levels σ by u^2_∞. In all the figures, the envelopes of the velocity vectors in the measurements planes which, in the following will be referred to as the streamline patterns are shown. The mean velocity components are presented only for the case R=2 as, for the other velocity ratios, appears qualitatively similar.

Figure 2a shows the streamlines and the mean streamwise (horizontal) velocity component contour at the symmetry plane of the jet. The map is in good agreement with that reported by Yuan et al. [5] and with data reported by Andreopoulos and Rodi [1]: in the proximity of the wall the cross-flow stagnates at the upstream side of the jet. Higher up, following the jet, as the cross-flow deflects over the jet, the flow accelerates. When the jet becomes strongly curved, its u velocity component assumes its maximum value at the location $x/D \cong 1$ in the jet trajectory, by approximately reaching one and a half times the value of the free stream velocity. Just downstream of the jet exit, the cross-flow fluid enters the jet wake creating a reverse motion, as it is clearly shown by the blue region which puts in evidence negative values of the u velocity component; at about 2 diameters downstream of the jet exit, the velocity becomes positive again.

Figure 2b shows the mean vertical velocity component v contour at the symmetry plane of the jet. There are only two regions with high v components: one which begins over the jet exit and is due to the high vertical momentum which accompanies the jet, the other one is located in the wake region where, according to Yuan et al. [5] there is a strong upward motion caused by the breakdown of the hanging vortices generated at the jet exit. Indeed, also the streamline pattern in that region puts in evidence the upward motion in the wake of the jet. As it can be seen from both strawberry-field figures 2a and 2b, downstream of the bending over region, the velocity component maximum are above the jet trajectories because of the acceleration of the free stream flow. The same considerations can be derived from figure 2c, in which the mean in-plane (z/D=0) total velocity $V = \sqrt{u^2 + v^2}$ contours are shown. Once again the maximum value is reached at the jet exit region, while minimum values can be found upstream and downstream of the jet; in the wake region, further downstream, the velocity seems to rise more rapidly at the location $y/D \cong 0.5$.

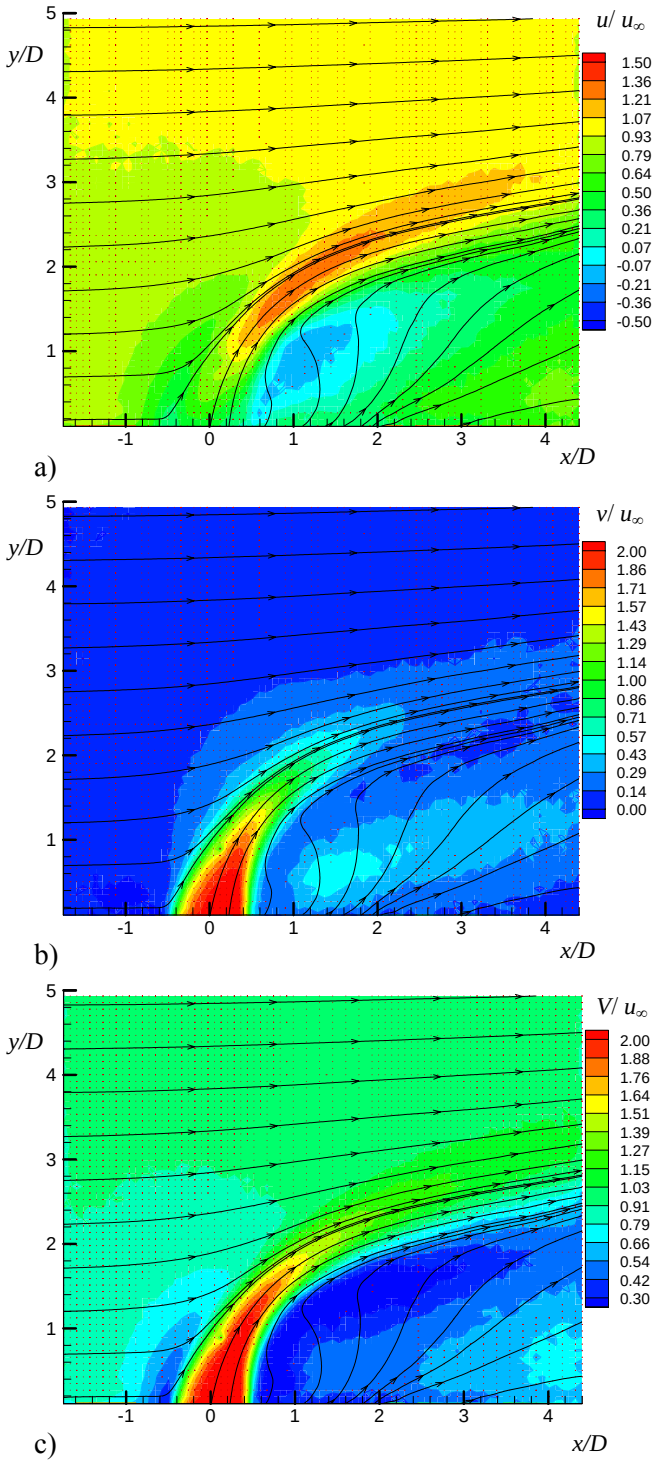

Fig. 2 In-plane streamlines at the centerplane z=0 for R=2: a) Mean streamwise velocity component u contours; b) mean vertical velocity component v contours; c) mean total velocity V contours.

In figure 3, the main turbulence statistics in the centerplane are reported for the velocity ratio equal to 2. Figure 3a shows the in-plane turbulent kinetic energy $\sigma=(\overline{u'^2} + \overline{v'^2})/u^2_\infty$ contours, while figure 3b shows the Reynolds stresses $\overline{u'v'}/u^2_\infty$ contours. The

maximum value of the turbulent kinetic energy is found in the same region where the u velocity component reached its highest values. The maximum is due to the high turbulence produced by the vortices and by the shear between the jet and the cross-flow.

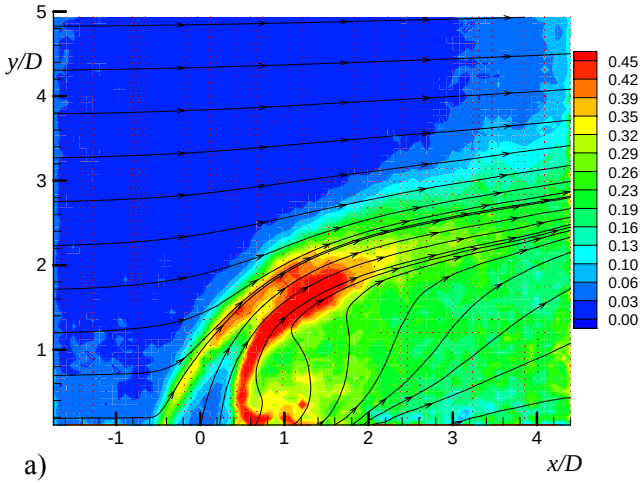

a)

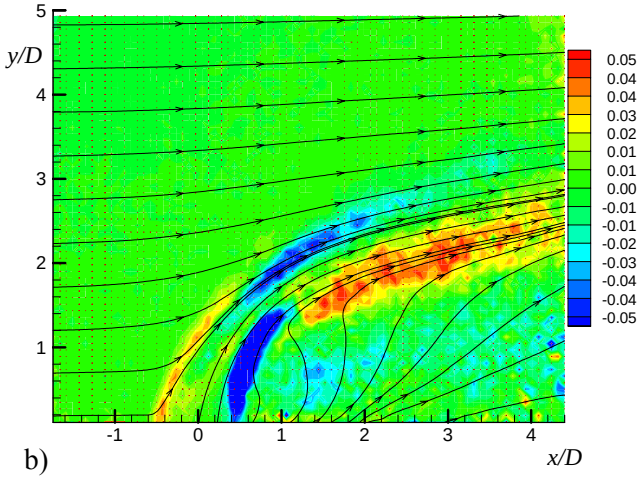

b)

Fig.3 Streamlines at the centerplane z=0 for R=2. a) In-plane (z=0) turbulent kinetic energy; b) contours of $\overline{u'v'}/u^2_\infty$.

In this case the maximum value is below the mean trajectory because of the additional contribution to turbulence of the counter rotating vortex pair. The measured values of the in-plane turbulent kinetic energy are in agreement with the map reported by Yuan et al. [5], even though the Reynolds number of the present work is quite higher and the out of plane turbulent kinetic energy is not measured. As it can be seen from figures 3b, Reynolds stresses $\overline{u'v'}/u^2_\infty$ are quite high in the regions with high velocity gradients, which are located in the vicinity of the jet exit and in the shear layer between the jet and the free-stream. In the wake region the shear stress is quite low, because of the smaller and more uniform velocity: the strong curvature generated by

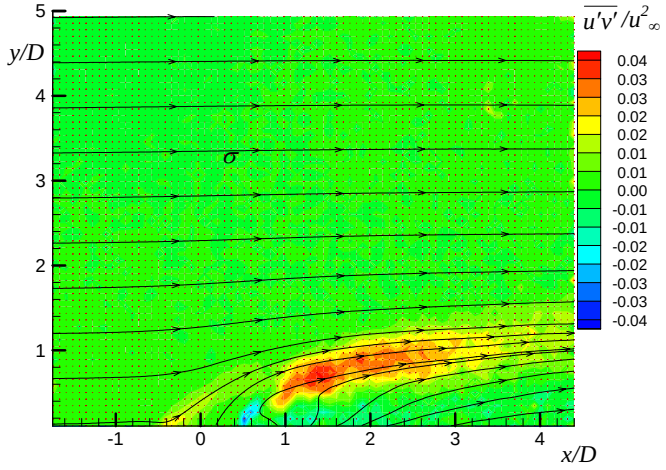

Fig.4 Streamlines at the centerplane z=0 for R=1. Contours of $\overline{u'v'}/u^2_\infty$.

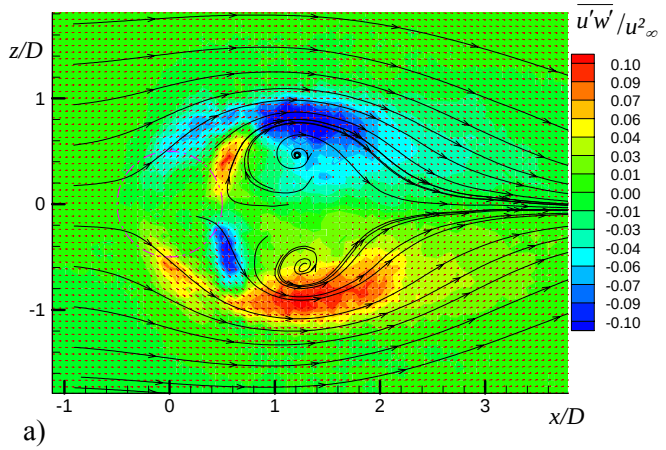

a)

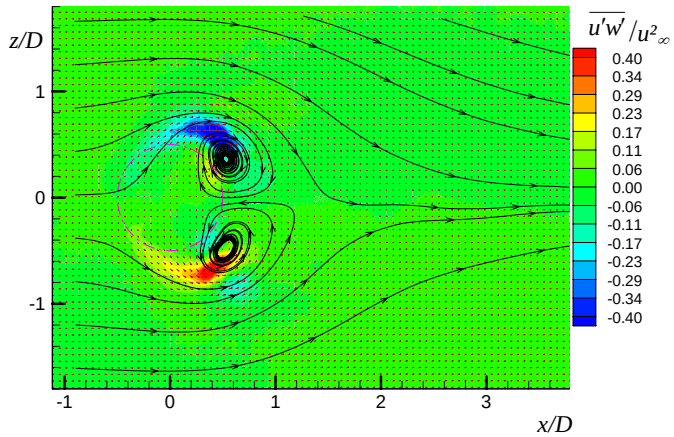

b)

Fig.5 Mean velocity field and contours of $\overline{u'w'}/u^2_\infty$ at the plane y/D=1: a) R=3; b) R=5.

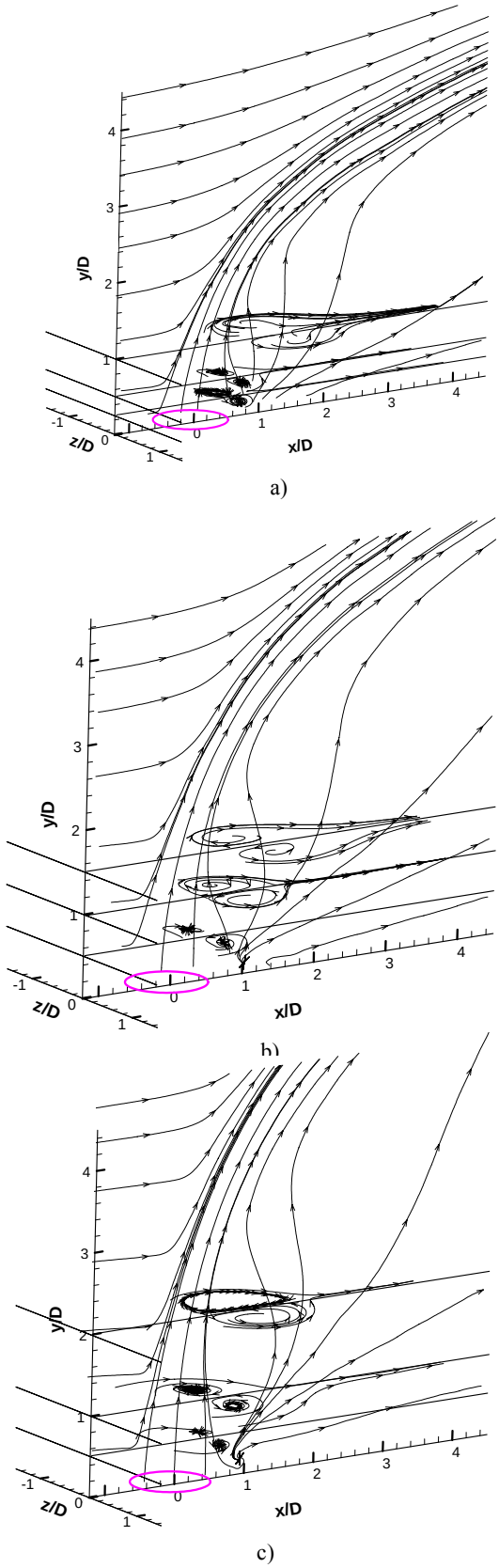

Fig.6 Composite mean streamline pattern: a) for R=3; b) R=4; c) R=5.

the interaction with the cross-flow has a stabilizing effect on the flow.

Figure 4 shows the streamlines at the symmetry plane for a value of the velocity ratio equal to 1; the turbulent shear stresses contour ($\overline{u'v'}$) are plotted in the background. This plot is reported in order to analyze the effect of R on the streamline pattern and on the shear stresses. In agreement with Kelso et al. [2] a node is visualized in the wake region near the wall at location $x/D \cong 1$ which can be more clearly seen as the velocity ratio increases. At higher R values the jet penetrates further into the cross-stream and the wake region gets larger generating a lower back pressure. This low pressure region, as it was mentioned before, causes an inflow towards the symmetry plane and the reverse flow near the node. During the tests, in the vicinity of the wall, the laser sheet reflection enhanced the noise and, as a consequence, it is not possible to measure, in this region, the velocity vectors in details. At high R values, the velocity distribution over the exit is more uniform and the jet bending over is more gradual. The small field of view did not allow to analyze the flow pattern for x/D >4, where there is a light downward motion of the jet and the flow near the wall assumes a boundary layer character. Furthermore, at higher velocity ratios the jet wake gets wider, and the low pressure region generates a stronger upward motion in order to remove the velocity deficit in the wake.

It is evident form the Fig. 3a that the turbulent stress has opposite sign in the upstream and downstream layer. In cases with $R>1$, downstream of the jet bent over, the turbulent stress profile changes sign three times instead of twice, because the streamwise velocity is higher than the freestream one. As the velocity ratio increases, the shear stress in the vicinity of the wall decreases since the jet exit streamlines are more uniformly distributed.

In the above reported maps no steady vortices could be seen in agreement with previous results: for the high Reynolds number adopted in the present tests, vortices generated in the near wall region are unsteady and move downstream of the jet exit, that's why they are visualized only in the instantaneous images.

In order to visualize the counter rotating vortex pair, tests are conducted in planes normal to the jet at different y/D distances. Figure 5 shows the in-plane streamlines and the contour maps of the turbulent shear layer $u'w'$ for R=3 and R=5 at the plane y/D=1; the other velocity ratios are qualitatively similar, and therefore not reported herein. The maximum values of the shear stress

correspond to the lateral edges of the jet, and there is a small region behind the jet where the stresses change sign, as it is shown in the figure. The counter rotating vortex pair moves upstream for increasing *R* and the vortices get smaller; as a consequence, also the region with the maximum values of the shear stresses moves upstream.

For *R*=1 and *R*=2, it was not possible to visualize these vortices, because they are too small and the bent over of the jet is much closer to the wall than for higher *R* values. For the cases *R*=3, *R*=4 and *R*=5, the steady vortex structures can be clearly seen from the 3D reconstructed flow of figure 6, in which the composite streamline pattern is reported. In the same figure the position of the jet exit is indicated with the purple circle. In all three cases moving along the jet, i.e. for increasing distance *y/D* the bound vortices become larger, and move not only downstream of the nozzle exit but also downstream of the jet itself.

Finally, in the present work, the following power law (Fig. 7) fit is proposed for the experimentally measured jet trajectory:

$$\frac{y}{RD} = A\left(\frac{x}{D}\right)^n \qquad (1)$$

The trajectory used for the fit is defined as the mean streamline originating from the center of the jet exit. The values of the computed coefficient *A* and exponent n are respectively 0,781 and 0,358 with a correlation factor r^2=0,9729. The functional form of eq. (1) reported by Camussi et al. [8]:

$$\frac{y}{D} = A\left(\frac{x}{D}\right)^n \qquad (2)$$

The last authors have found two linear fits with different slopes of *A(R)* for *R*<2 and *R*>2. In the present case, as shown in figure 8, a very good homogeneous linear fit (r^2=0,9998) of *A* as a funciotn of *R* exists, and this explains the form of the proposed correlation (eq. (1)). The different behavior may be due to the much higher Reynolds number adopted in the present work.

4. Conclusion

In this paper PIV measurements of the velocity field of a jet in cross-flow are presented; the results are compared with measurement made by other authors. In particular there is a quite good agreement with data presented by Andreopoulos and Rodi [1] and by

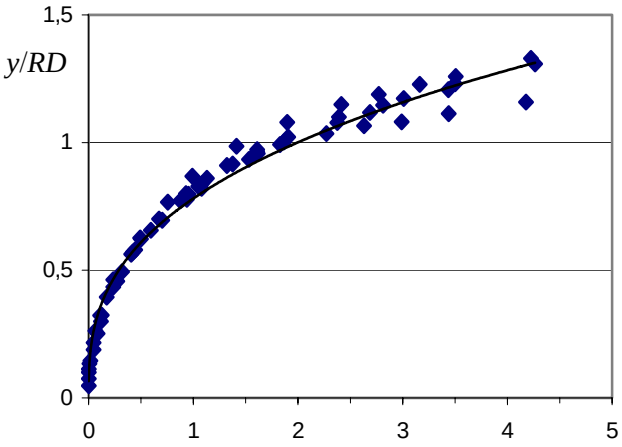

Fig.7 Power law fit of the jet trajectory.

Yuan et al. [5] Measurements are performed in the symmetry plane of the jet and in planes normal to it by varying the jet to free-stream velocity ratio from 1 to 5

In the symmetry plane, all the visualized vortices are unsteady, so they do not appear in the mean flow pattern. In the plane normal to the jet, the steady counter rotating bound vortex pair can be clearly seen behind the jet only for high velocity ratios. One nozzle diameter downstream of the jet core a node with a reversed flow region is present for all the tested values of *R*; at high *R* the reversed flow zone gets wider and the low pressure region generates a stronger upward motion in order to remove the velocity deficit in the wake. Reynolds shear stresses $\overline{u'v'}/u^2_\infty$ are quite high in the regions with high velocity gradients, which are located in the vicinity of the jet exit and in the shear layer between the jet and the free-stream. In the wake region the shear stress is quite low, because of the lower and more uniform velocity there.

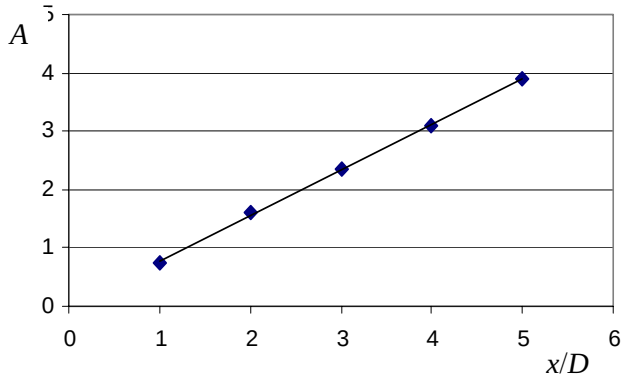

Fig.8 Linear fit of *A(R)*.

As expected from symmetry considerations, the shear stresses $\overline{u'w'}/u^2_\infty$ are zero at the symmetry plane and assume opposite values at the lateral edges of the jet. By making measurements at various distances from the wall, it is possible to evidence the composite mean streamline pattern at different velocity ratios and to analyze the behavior of the counter rotating vortex pair. Vortices in the lee edge and in the wake region of the jet are observed, while no horseshoe vortex is detected because of the high value of the Reynolds number. For all the velocity ratios, vortex rings are observed on the upstream and downstream edges of the jet in the instantaneous velocity fields. An original fit with a high correlation factor is also proposed for the mean jet trajectory.

References:

[1] Andreopoulos, J. and Rodi, W. Experimental investigation of jets in a cross flow. *J. Fluid Mech.* 1984 Vol. 138, 93-127.

[2] Kelso, R. M., Lim, T.T. and Perry, A. E. An experimental study of round jets in cross-flow. *J. Fluid Mech.* 1996 Vol. 306, 111-144.

[3] Sykes, R. I., Lewellen, W. S.and Parker, S. F. On the vorticity dynamics of a turbulent jet in a crossflow. *J. Fluid Mech.* 1986 Vol. 168, 393-413.

[4] Coelho, S. R. M. and Hunt, J. C. R. The dynamics of the near field of strong jets in cross-flow. *J. Fluid Mech.* 1989 Vol. 200, 95-120.

[5] Yuan, L. L., Street, R. L. and Ferziger, J. H. 1999 Large-eddy simulations of a round jet in crossflow. *J. Fluid Mech.* 1999,Vol. 379, 71-104.

[6] Meyer, K. E., Özcan, O. and Westergaard, C. H. Flow mapping of a jet in crossflow with stereoscopic PIV. Fourth International Symposium on Particle Image Velocimetry, September 17-19m, 2001 , Göttingen, Germany.

[7] Somerscales, E. F. C. Fluid velocity measurement by particle tracking. Flow, its *Measurements and Control in Science and Industry*. 1980 Vol. I, pp. 795-808.

[8] Camussi, R., Guy, G. and Stella A. Experimental study of a jet in a crossflow at very low Reynolds number. *J. Fluid Mech.* 2002 Vol. 454, 113-144.